

The Procyon Campaign: Frequency Analysis and Maximum Likelihood Estimation of Mode Parameters

T. L. Campante^{1,2}, H. Kjeldsen², T. R. Bedding³, M. J. P. F. G. Monteiro¹

¹ Faculdade de Ciências & Centro de Astrofísica da Universidade do Porto, Porto, Portugal; e-mail: campante@astro.up.pt
² Danish Asteroseismology Centre, Department of Physics and Astronomy, University of Aarhus, Aarhus, Denmark
³ Institute of Astronomy, School of Physics, University of Sydney, Sydney, Australia

Abstract. A multi-site campaign to measure solar-like oscillations in the F5 star Procyon A was carried out from 2006 Dec 28 until 2007 Jan 23, employing eleven telescopes at eight observatories. A set of *ad hoc* weights intended to optimize the spectral window was adopted in the calculation of the combined power spectrum. Iterative Sine-Wave Fitting (ISWF) was applied in extracting candidate modes of oscillation and two distinct ridges could be established in an échelle diagram. An unambiguous identification of the ridges was attempted after applying a likelihood ratio test. In order to do so, a regularized Maximum Likelihood (ML) procedure, comprising prior constraints, was employed in fitting the power spectrum. As a result, best-fitting mode parameter estimates (frequencies, mode heights, linewidths) and their formal uncertainties were retrieved. The issue concerning the evolutionary state of Procyon is mentioned.

1. Introduction

For more than 15 years several groups have studied the solar-like oscillations in Procyon A, though with no agreement on the actual eigenfrequencies. This was probably due to either aliasing or short mode lifetimes. A spectroscopic multi-site campaign using 11 telescopes worldwide with a time span of nearly 4 weeks was performed to identify frequencies and determine the stellar properties and evolutionary state. We are one of several groups working on the data. Here we show some preliminary results from our analysis.

2. Preliminary Frequency Analysis

Aimed at obtaining an estimate of the large separation, $\Delta\nu$, and initial guesses for the mode frequencies, thus setting out the ML approach.

2.1. Sidelobe-Optimized Power Spectrum

Even with almost continuous coverage for the central 10 days, velocity precision varies greatly both for a given telescope and from one telescope to another. A general algorithm for adjusting the weights in order to minimize the sidelobes in the spectral window has been developed and tested on published data on α Cen A and B, and β Hyi [2]. This method was applied in the present case, where prominent sidelobes at $\pm 11.57 \mu\text{Hz}$ could be seen (Fig. 1). In brief, we adjusted the weights as a means to remove the inhomogeneous density character of the time series data.

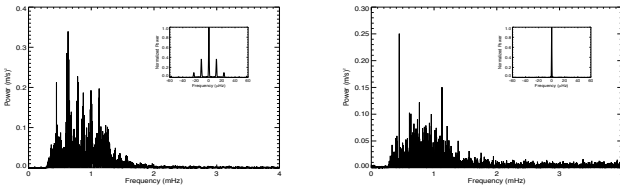


Figure 1: *Left Panel:* Noise-optimized power spectrum as obtained in [1]. *Right Panel:* Sidelobe-optimized power spectrum. Insets show the corresponding spectral windows.

2.2. Autocorrelation and ISWF

Autocorrelation of the sidelobe-optimized power spectrum was performed within the range 0.5-1.5 mHz. An estimate of the average large separation of $\sim 55.3 \mu\text{Hz}$ was thus retrieved. ISWF makes clear the presence of 2 distinct ridges in an échelle diagram (Fig. 2). Fitting a polynomial to one of the ridges, e.g. the leftmost, and assuming one of the two possible identification scenarios as well as the asymptotic relation, one may obtain a set of initial guesses for the mode frequencies. Reversing the assumed identification, a complementary set of guesses is acquired.

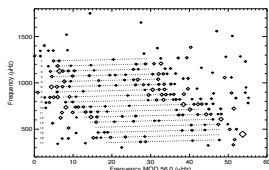


Figure 2: Échelle diagram displaying 200 (default) extracted candidate modes. Symbol size is proportional to the S/N .

3. Maximum Likelihood Estimation

To be precise, we employed a regularized version of ML estimation, including prior constraints, i.e. Maximum A Posteriori (MAP). The latter is a Bayesian approach as opposed to the Fisherian character of the former.

3.1. Fitting the Power Spectrum: Implementation

- Global fitting strategy: 17 orders over the range 300-1300 μHz
- 3 central frequencies per order, corresponding to $l = 0, 1, 2$ -modes
- Mode peaks described by symmetric Lorentzian profiles
- Model convolved with transfer function: allow for windowing/weighting
- Bins set 0.69 μHz apart: avoid oversampling and bin-to-bin correlations
- A single height parameter, H , per order; ratios of the mode heights given according to Table 1 of [4]
- Relative amplitudes within non-radial multiplets described by intensity visibilities [3]; inclination angle, i , fixed at 31.1° (binary orbit's inclination)
- A single linewidth parameter, Γ , per order
- Non-radial modes assumed to show symmetric rotational splitting: ν_s fixed either at 1.10 μHz ($P_{\text{rot}} = P_{\text{slow}}$; see [1]) or 0.55 μHz ($P_{\text{rot}} = 2P_{\text{slow}}$)
- Background modelled by flat component (photon shot noise)
- Power from $l = 3$ -modes included in some fits according to asymptotics
- 2 possible ridge identifications, namely scenario A (radial mode at $\sim 985 \mu\text{Hz}$) and scenario B ($l = 1$ -mode at $\sim 985 \mu\text{Hz}$)

3.2. Bayesian Constraints

- We chose the prior for the linewidths $\{\Gamma_i\}$ to be independent log-normal distributions [6]
- Based on Figures 13 and 14 of [5], we chose the prior for the small spacings $\{\delta\nu_{02,i}\}$ to be independent Gaussians with a mean of 4 μHz and a standard deviation, λ , that could take the values 3, 4 and 5 μHz

3.3. Results

Fit	Scenario	ν_s (μHz)	λ (μHz)	$l = 3$ -modes included	$-\ln(L)$	ϵ
MAP_1	A	0.55	4	Yes	-4875.0	0.026
MAP_2	A	0.55	3	Yes	-4873.7	0.026
MAP_3	A	0.55	5	Yes	-4876.7	0.026
MAP_4	A	1.10	4	Yes	-4876.3	0.029
MAP_5	B	0.55	4	Yes	-4879.1	0.034
MAP_6	B	0.55	3	Yes	-4875.0	0.034
MAP_7	B	0.55	5	Yes	-4872.3	0.034
MAP_8	B	1.10	4	Yes	-4870.3	0.035
MAP_9	A	0.55	4	No	-4877.4	0.016
MAP_10	A	1.10	4	No	-4875.3	0.018
MAP_11	B	0.55	4	No	-4872.3	0.035
MAP_12	B	1.10	4	No	-4868.8	0.036

Table 1: The 12 fits performed. L is the maximized likelihood. ϵ is defined in [5], which they state allows distinguishing between MS and evolved models, as well as does the behaviour of $\delta\nu_{01}$ (predicted to decrease with frequency for MS and to increase with frequency for PoMS).

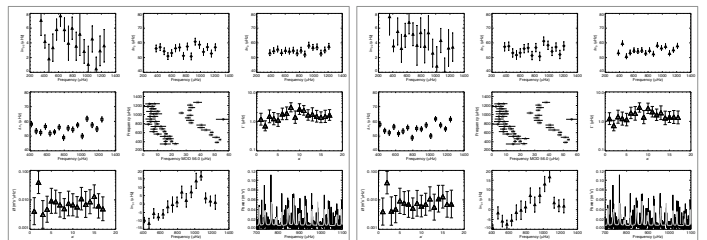


Figure 3: Series of plots concerning fits MAP_11 (*Left Panel*) and MAP_12 (*Right Panel*). For each Panel, from Top to Bottom and from Left to Right: $\delta\nu_{02}(\nu)$, $\Delta\nu_2(\nu)$, $\Delta\nu_1(\nu)$, $\Delta\nu_0(\nu)$, échelle diagram, $\Gamma(\nu^*)$, $H(\nu^*)$, $\delta\nu_{01}(\nu)$, fitting window excerpt.

4. Final Remarks

- Blending of components within multiplets strongly correlates i with ν_s
- Robustness of central frequency estimates regarding ν_s
- Need for Monte Carlo simulations, and MCMC techniques that would allow looking in detail at distributions of best-fitting parameters
- Likelihood ratio tests are inconclusive regarding ridge identification
- Alternative ID strategy: *near-surface effect correction* as a discriminator?
- Scenario B: $\delta\nu_{02}$ seems to follow similar trend to that predicted by models
- Scenario A: dependence on ϵ and the behaviour of $\delta\nu_{01}$ with frequency, seems to favour MS models; Scenario B then favours PoMS models
- Alternative prior for $\{\delta\nu_{02,i}\}$: the mean may be replaced by other values

[1] Asteroseismology, H. Kjeldsen, T. R. Bedding, T. R. Bedding, T. R., et al. 2006, *A&A*, 467, 1199
[2] Asteroseismology, H. Kjeldsen, T. R. Bedding, T. R., et al. 2009, *in Solar-stellar dynamics as traced by helio- and asteroseismology*, Proc. IAU Symposium 260, in press
[3] Gizon, L., & Belkacem, K. 2001, *A&A*, 369, 1009
[4] Kjeldsen, H., Bedding, T. R., Asteroseismology, T. R., et al. 2008, *A&A*, 482, 1370
[5] Pritzl, J., Bedding, T. R., Asteroseismology, T. R., et al. 2006, *A&A*, 460, 730
[6] Trampedach, R., & Appourchaux, P. 1994, *A&A*, 289, 649